β^- decay of the neutron-rich isotope ^{215}Pb

H. De Witte,[1,*] S. Eeckhaudt,[1] A. N. Andreyev,[2,†] I. N. Borzov,[3,‡] J. Cederkäll,[4] A. De Smet,[1] D. V. Fedorov,[5] V. N. Fedoseyev,[4] S. Franchoo,[4,§] M. Górska,[1,‖] H. Grawe,[6] G. Huber,[7] M. Huyse,[1] Z. Janas,[8] U. Köster,[4,¶] W. Kurcewicz,[8] J. Kurpeta,[8] A. Płochocki,[8] K. Van de Vel,[1] P. Van Duppen,[1] and L. Weissman[4]

[1]*Instituut voor Kern- en Stralingsfysica, KU Leuven, University of Leuven, B-3001 Leuven, Belgium*

[2]*University of Liverpool, Liverpool L697ZE, United Kingdom*

[3]*Bogoliubov Laboratory of Theoretical Physics, Joint Institute for Nuclear Research, 141980 Dubna, Russia*

[4]*CERN ISOLDE, CH-1211 Genève 23, Switzerland*

[5]*Petersburg Nuclear Physics Institute, RU-188350 Gatchina, Russia*

[6]*GSI, D-64291 Darmstadt, Germany*

[7]*University of Mainz, D-55099 Mainz, Germany*

[8]*Faculty of Physics, University of Warsaw, Hoza 69, PL-00681 Warsaw, Poland*

(Received 26 March 2013; published 7 June 2013)

This Brief Report reports on the first observation of the β^--delayed γ decay of ^{215}Pb, feeding states in ^{215}Bi. The ^{215}Pb beam was produced using resonant laser ionization and mass separated at the ISOLDE-CERN on-line mass separator. This ensured clean identification of the γ rays as belonging to the decay of ^{215}Pb or its β-decay daughters. A half-life of 147(12) s was measured for the ^{215}Pb β decay and a level scheme for the daughter nucleus ^{215}Bi is proposed, resulting in an extended systematics of the excited states of the neutron-rich Bi isotopes.

DOI: 10.1103/PhysRevC.87.067303 PACS number(s): 21.10.Tg, 23.20.Lv, 23.40.−s, 27.80.+w

Despite the wealth of experimental data available for the doubly magic nucleus ^{208}Pb ($Z = 82, N = 126$) and its closest neighbors, the more neutron-rich lead isotopes remain poorly explored. The reason for the limited spectroscopic information lies in the experimental difficulties to access this region of the nuclear chart. Indeed the high N/Z ratio of these isotopes rules out heavy-ion fusion-evaporation reactions to produce the nuclei of interest and spallation reactions suffer from high contamination levels from more abundantly produced isobars.

However, over the last years other techniques have been used to explore this region east of ^{208}Pb. Deep-inelastic scattering reactions populated high-spin states in $^{208-210}$Pb [1–3] and ^{211}Bi [4], yielding information on single-particle states and their coupling to collective modes. At FRS-GSI Pfützner *et al.* [5] identified eight previously unobserved isotopes with $Z = 80$–84 in the fragmentation of a 1 GeV/nucleon ^{238}U beam. In the lead isotopic chain, ^{215}Pb was observed for the first time; bismuth isotopes up to $A = 218$ were identified. More recently, 40 new neutron-rich isotopes around $Z = 82$, including $^{215-220}$Pb, were identified with the same technique [6], isomeric decays in very neutron-rich lead isotopes were studied up to ^{216}Pb [7] and life times for a number of β-decaying isotopes were reported [8].

At ISOLDE [9] spectroscopic studies of $^{215-218}$Bi and ^{215}Pb decay have been carried out successfully. The combination of the resonance ionization laser ion source (RILIS) [10,11] and the pulsed release method [12], have paved the way to reach these isotopes, by efficiently suppressing the otherwise huge isobaric contamination. In this Brief Report we present the results of a β^--decay study of ^{215}Pb. The results for the isomeric and/or β decay of $^{215-218}$Bi [13–16] for which data were collected during the same experimental campaign have been reported elsewhere.

The β^- decay of ^{215}Pb has been observed at ISOLDE in a high-energy proton induced spallation reaction. A 1.4 GeV pulsed proton beam bombarded a thick (50 g/cm^2) UC$_x$ target. The proton beam, with an intensity of 3.1×10^{13} particles per pulse was delivered by the PS booster, during a 16.8 s long supercycle, made of 14 equidistant pulses, 1.2 μs long each. Out of these 14 pulses, seven were sent to the ISOLDE target. After diffusion out of the target, the spallation products were selectively ionized in the resonance ionization laser ion source [10,11]. The element-selective laser ionization of the lead isotopes in the hot niobium cavity (2100 °C, 3 mm diameter, 30 mm length) was achieved in three steps: after doubling of the fundamental frequency in a nonlinear BBO (β barium borate) crystal, a tunable pulsed dye laser delivered a photon beam with a wavelength $\lambda = 283.305$ nm to raise a valence electron out of the $6p^2(1/2,1/2)_0$ ground state to a first excited atomic state $6p7s(1/2,1/2)_1$. For the second step, the wavelength of the second dye laser was tuned to 600.186 nm, thus exciting the atoms to a $6p8p(1/2,3/2)_2$ state. The copper-vapor lasers, pumping the dye lasers, simultaneously provided the necessary energy for the final ionizing step.

Subsequently, the ions were extracted by a 60 kV extraction voltage and mass separated by the ISOLDE-GPS separator. After every proton impact, the beam-gate was closed for 100 ms reducing the isobaric contamination, lowering the amount of

*Hilde.DeWitte@fys.kuleuven.be

†Present address: Department of Physics, University of York, York YO10 5DD, UK.

‡ExtreMe Matter Institute EMMI, GSI Helmholtzzentrum für Schwerionenforschung, Planckstraße 1, 64291 Darmstadt, Germany.

§Present address: Institut de Physique Nucléaire d'Orsay, F-91406 Orsay Cedex, France.

‖Present address: GSI, D-64291 Darmstadt, Germany.

¶Present address: Institut Laue-Langevin, BP 156, 6, rue Jules Horowitz, 38042 Grenoble Cedex 9, France.

short-lived, surface-ionized elements, like the francium α emitters with respect to the longer-lived β-decaying lead isotopes. This method, known as pulsed release, is discussed in [12].

Finally, the ions reached the detection setup and were implanted onto a movable aluminized mylar tape (thickness 100 μm and width 12.5 mm). Separate implantation and decay positions were used: the activity was implanted for 16 supercycles (268.8 s) and then transported towards a well shielded decay station where the radioactive decay was measured for the same period.

Two HPGe detectors (75% and 70% relative efficiency) and one low-energy germanium detector (LEGe), in close geometry, provided the γ-ray information at the decay station. A 1 mm thick plastic (NE102A) ΔE detector of 31 $\times$ 25 mm^2, installed in front of the LEGe detector, detected the β particles with an efficiency of 8(1)%. Data were taken simultaneously in multiscaling mode (8 $\times$ 32.85 s) and event-by-event, so-called list mode. Any two detectors firing simultaneously triggered the list-mode acquisition.

The element selectivity of the resonance ionization laser ion source provided an essential identification technique for the study of the ^{215}Pb β^- decay. Comparing the spectra taken with and without laser ionization in the ion source, reveals the ^{215}Pb related γ rays and the daughter activities. Data were collected for 16 h with the lasers resonantly tuned for lead ionization and for 5 h without laser ionization. Figure 1 shows the on- and off-resonance β-gated γ spectra obtained with the LEGe detector. The γ ray at 183.5(3) keV, present only in the on-resonance spectrum is assigned to the β^- decay of ^{215}Pb. The resonant line at 293.7 keV was known to be the strongest γ line belonging to the β decay of ^{215}Bi [17]. The main background lines (present in both laser-on and laser-off spectra) are assigned to the lighter francium isotopes (e.g., ^{212,213}Fr) and their daughters. They are abundantly produced by spallation of uranium and, due to their low ionization potential (4.07 eV) are easily surface ionized in the hot cavity of the ion source. The yields of these beams are about ten orders of magnitude higher compared to ^{215}Pb, hence even if only a tiny fraction passes the mass separator, they will be observable.

Additionally, γ rays from the ^{84m}Br β decay (424.0, 881.6, 1462.8 keV) are observed in the spectra. These are most probably due to diatomic molecular beams resulting from radiogenic production of both components [18], in this case ^{131g}Ba and ^{84m}Br. The long lifetime of the former ($T_{1/2} = 11.50$ d) allowed it to accumulate in the target system but also prevented the observation of its characteristic γ rays in the spectrum.

The inset in Fig. 1 shows the time behavior of the 183.5 keV γ ray. From a fit with a single-component exponential function of both multiscaling and list mode data sets, a weighted average for the ^{215}Pb β-decay half-life was determined to be 147(12) s.

Weaker transitions, not observed in the total β-gated γ-ray spectra, were found in coincidence with the 183.5 keV line and were ascribed to the ^{215}Pb decay on the basis of this coincidence relation and the coincidence with bismuth Kx rays. The spectrum gated on the 183.5 keV transition is shown in Fig. 2. The four γ-ray transitions observed between 1300 and 1450 keV could not be firmly assigned to the ^{215}Pb decay because of the absence of coincident Bi x rays and observed coincidences with contaminant γ rays.

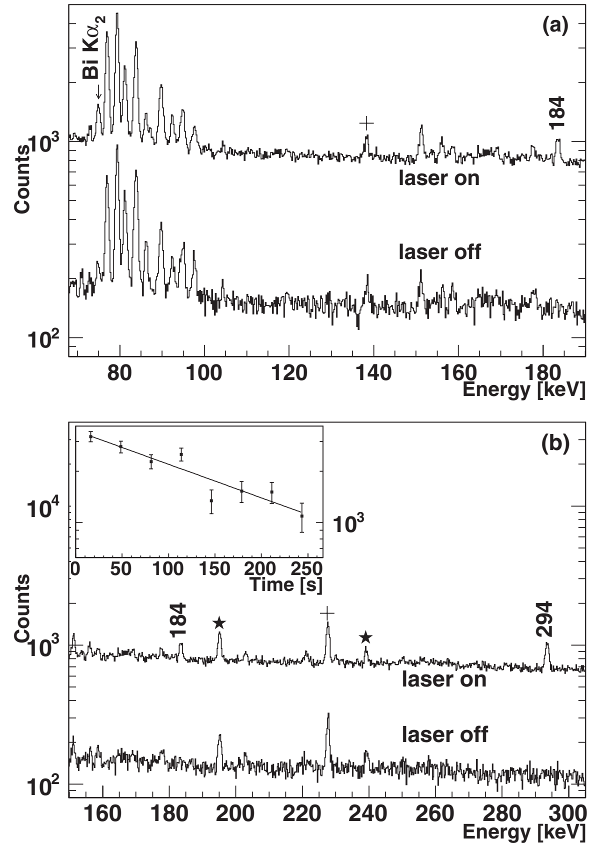

FIG. 1. β-gated γ-ray spectrum collected with the LEGe detector obtained for mass $A = 215$, laser on-resonance (upper spectrum) vs. off-resonance (lower spectrum). The energy range from 70 to 300 keV is shown in the two spectra (a) and (b). The spectra are not counting-time matched. The lines marked with * belong to ^{209}At EC decay and those with + to the ^{212}Fr decay. The γ ray at 151 keV is not identified, but is present both in the on- and off-resonance spectra. The inset shows the time behavior of the 184 keV line, from the ^{215}Pb β decay, in the eight consecutive time bins of the multiscaling mode.

Energies and relative γ-ray intensities, not corrected for true summing effects, are listed in Table I. The intensities are corrected for the detection efficiency that was calculated using GEANT simulations [19]. Based on the coincidence relations a level scheme is proposed as shown in Fig. 3.

TABLE I. Energies, relative intensities (normalized to the strongest γ ray), area of the peak in the spectrum gated on the 183.5 keV γ ray, and coincidence relations for the γ transitions following the ^{215}Pb β^- decay.

Energy [keV]	$I_{\rm rel}$ [%]	Area	Coincident γ lines
183.5(3)	100(19)		671, 760, 839, 985, 1016, 1327
671(1)	14(5)	45(13)	Bi Kx, 184
760(1)	12(5)	36(11)	Bi Kx, 184, 1016, 1200
839(1)	21(7)	59(12)	Bi Kx,184
985(1)	24(8)	59(13)	Bi Kx, 184
1016(1)	14(5)	35(10)	184,760
1200(1)	17(11)		760

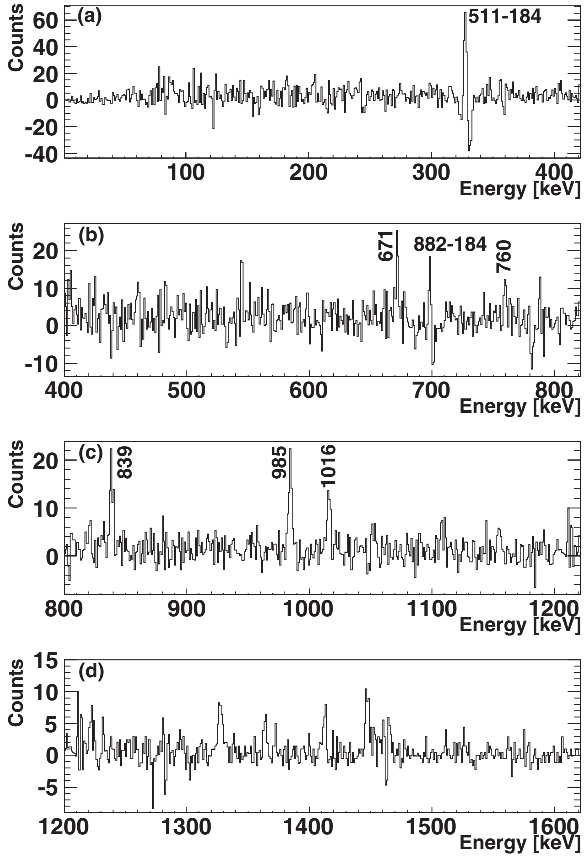

FIG. 2. Background corrected γ-ray spectrum gated on the 183.5 keV γ ray attributed to the ^{215}Pb β^- decay. The energy range from 0 to 1600 keV is shown in the four subsequent spectra (a)–(d). The lines at 1327, 1364, 1412, and 1447 keV could not be firmly assigned to the ^{215}Pb decay. The lines at (511–184) keV and (882–184) keV arise from the Compton scattering of the intense γ rays at 511 and 882 keV, respectively.

The relative intensities of the 183.5 keV γ ray and the Bi $K\alpha_2$ x rays in the spectra gated on 760, 839, and 985 keV were used to determine the internal conversion coefficient for the 183.5 keV transition $\alpha_K = 1.2(4)$. Comparison with theoretical α_K values (0.08 for $E1$, 1.54 for $M1$, and 0.21 for $E2$ [22]) shows that the transition is of dominant $M1$ type. A similar conversion coefficient of 1.4(3) was also determined from the total β-gated spectrum assuming all observed Kx rays originate from the conversion of the 183.5 keV transtion. This indicates that no additional strongly converted lines are present in the decay of ^{215}Pb.

The ground state β-decay feeding in ^{215}Bi was determined by comparing the intensities of the 183.5 keV γ ray and the 293.5 keV γ ray in the daughter decay. Corrections were made for γ-detection efficiency and for the measurement cycle (a function of the half-lives, accounting for the fraction of nuclei implanted on the tape but not decayed in front of the detector during the measurement time). The absolute γ-ray intensity of the 293.5 keV line was taken from [13] [$I_\gamma = 35.2(11)\%$]. Taking into account the internal conversion coefficient of $\alpha_K = 1.2(4)$ for the 183.5 keV line, an apparent β-decay ground state feeding of 81(4)% was deduced. This value represents only an upper limit for the ground state feeding, because of possibly unobserved γ rays from higher-lying states directly decaying to the ground state.

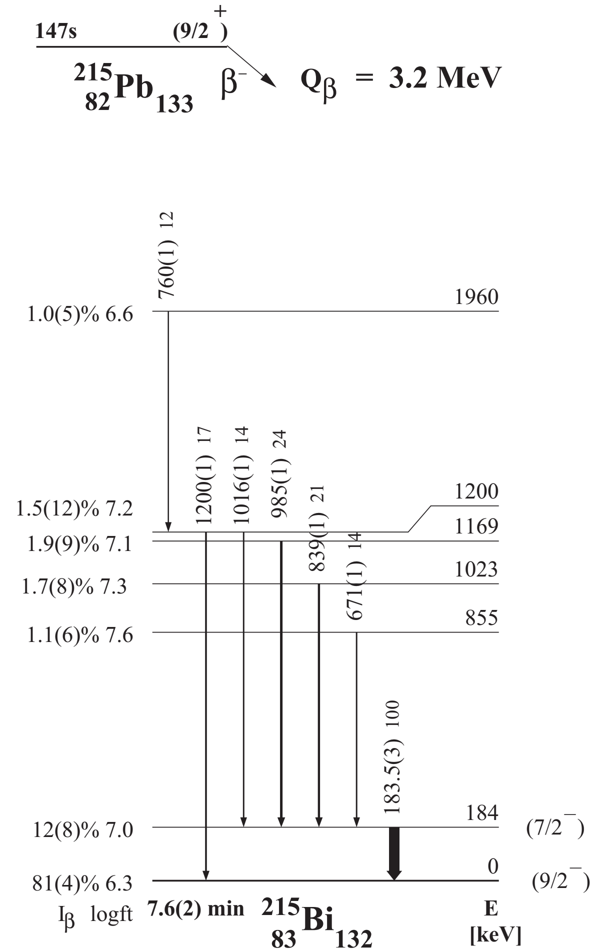

FIG. 3. Proposed decay scheme of the β^- decay of ^{215}Pb. The $Q_\beta$value is taken from [20]. The ^{215}Bi half-life is taken from [21]. Potentially γ rays from unidentified higher-lying states that decay towards the ground or the excited states, were not observed in this study. Therefore the reported β-feeding probabilities and $\log ft$ values should be considered as upper and lower limits.

The obtained half-life of ^{215}Pb [$T_{1/2} = 147(12)$ s] is in good agreement with our prediction (165 s) from a self-consistent density functional plus continuum-QRPA framework [23]. In the present work we have performed a new calculation based on the same DF3 functional but with the use of the effective particle-hole interaction parameters found from the analysis of nuclear magnetic moments in [24]. The odd neutron in ^{215}Pb and the odd proton in ^{215}Bi have been fixed (before variation) in the $9/2^+$ and $9/2^-$ orbitals, respectively. Accounting in such a way for the evaluated spins and parities of the parent and daughter ground states, one comes to the half-life of 185 s. An important feature of the calculated β-strength function is the absence of the Gamow-Teller decays within the Q-window. The lowest GT excitation in the daughter nucleus is mostly related to the $(\nu 1i_{11/2}, \pi 1i_{13/2})$ transition involving the partially filled neutron $\nu 1i_{11/2}$ level (the calculated occupancy factor is 0.41). As the corresponding

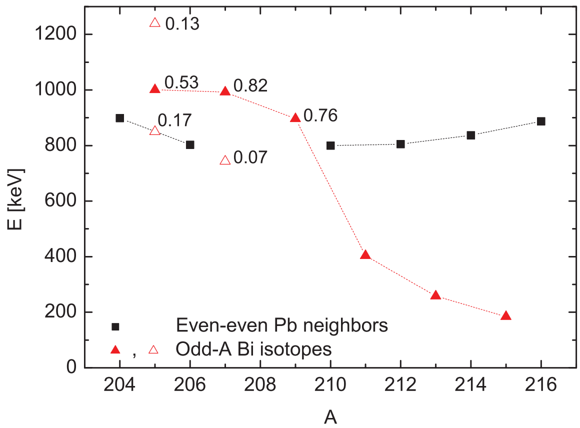

FIG. 4. (Color online) Energy systematics for the lowest-lying $7/2^-$ levels in the odd-A bismuth isotopes, along with the energy of the first 2^+ state in the underlying even-even lead core. Data are taken from [7,21]. Below $A = 211$ the line connects the levels carrying the main $\pi f_{7/2}$ strength. The spectroscopic factors from Pb(α,t), taken from [21], are shown next to the data points when known. For $A \geqslant 211$, the lowest lying levels are connected.

quasiparticle transition energy (2.76 MeV) is higher than the $Q_\beta(DF3) = 2.26$ MeV, the calculated total β-decay half-life is entirely due to the first-forbidden decays. The existence of an analogous β-decay pattern near the $N = 126$ neutron shell has been discussed for ^{204} Pt [25,26].

The new experimental data do not allow to extract direct information on the spin and parity of the ground state of ^{215}Pb or ^{215}Bi, but on the basis of systematics spin and parity $I^\pi = 9/2^+$, respectively, $I^\pi = 9/2^-$ can be expected for ^{215}Pb and ^{215}Bi. The $9/2^+$ ground state of the ^{215}Pb parent nucleus would correspond to the odd neutron occupying the $\nu 2g_{9/2}$ orbital. The ^{215}Bi daughter has one proton outside the $Z = 82$ core most probably occupying the $\pi 1h_{9/2}$ orbital which would result in a $9/2^-$ ground state. The β^- decay proceeds mainly to the ^{215}Bi ground state [81(4)%] and to the first-excited state at 183.5 keV [12(8)%] albeit with a log ft value consistent with a first forbidden transition [27].

The first-excited state is given a tentative $7/2^-$ assignment on the basis of the $M1/E2$ character of the 183.5 keV transition, the log ft value and the systematics in the lighter Bi isotopes. In the semimagic ^{209}Bi the first-excited state corresponds to the 83rd proton occupying the $\pi 2f_{7/2}$ orbital. This assignment is also kept for the heavier isotopes, where it is supported by the high hindrance factors in the α decay of the ^{215,217}At ground state $(\pi 1h_{9/2}^3, \nu 2g_{9/2}^{4,6})$ towards the first-excited state in the Bi daughters (HF = 380 [21] and HF = 500 [28] for ^{215}At and ^{217}At). The availability of laser ionized At beams at ISOLDE [29] could allow a further exploration of this decay pattern in the heavier isotopes.

The energy of the lowest lying $7/2^-$ levels with respect to the $9/2^+$ ground state in the odd-A bismuth isotopes is presented in Fig. 4, together with the energy of the first-excited 2^+ states in the neighboring lead isotopes.

At the $N = 126$ shell closure (^{209}Bi) the $7/2^-$ level, situated at 896 keV, carries the major part of the $\pi 2f_{7/2}$ single-particle strength. Towards the neutron-deficient side close lying $7/2^-$ levels were identified. One-proton transfer reaction studies on the underlying $^{(A-1)}$Pb core show that the $7/2^-$ levels at 1001 keV and 992 keV in ^{205}Bi and ^{207}Bi carry most of the proton $\pi 2f_{7/2}$ single-particle strength [30]. The lower level has been interpreted as the $7/2^-$ member of the multiplet from the coupling of the $\pi 1h_{9/2}$ proton with the 2^+ state in the underlying $^{(A-1)}$Pb core. The energy of the first excited $7/2^-$ level drops steeply when neutrons are being added beyond $N = 126$. The anomalously low-lying $7/2^-$ state was assumed to arise from the particularly strong coupling of the $\pi 2f_{7/2}$ single-proton state and the $7/2^-$ member of the $i_{13/2} \otimes {}^{208}$Pb($3^-$) core coupling state as shown in the calculations of [31]. However, this interpretation was weakened by ^{208}Pb(α,p) transfer reaction studies [32], where it was shown that the $7/2^-$ level in ^{211}Bi carries still 52% of the $\pi 2f_{7/2}$ strength.

Monopole energy shifts of single-particle levels have been observed in other mass region [33–35] and a similar problem related to an anomalous low-lying $5/2^+$ state in ^{135}Sb has been explained by recent shell-model calculations [36]. Similar calculations in the ^{208}Pb region have been initiated [37]. It will be interesting to compare our recent findings with these or other shell-model calculations.

Final conclusions on the single-particle strength of the proton orbitals in the bismuth isotopes could be drawn from, e.g., (α,t) transfer reaction studies using radioactive beams of the respective even-even lead isotopes. These experiments should become possible with the availability of HIE-ISOLDE.

This work has been funded by FWO-Vlaanderen (Belgium), by GOA/2010/010 (BOF KU Leuven), by the Interuniversity Attraction Poles Programme initiated by the Belgian Science Policy Office (BriX network P7/12), and by the European Commission within the Seventh Framework Programme through I3-ENSAR (contract no. RII3-CT-2010-262010). I.B. is partially supported by Helmholtz Alliance EMMI and the grant by IN2P3-RFBR under agreement no. 110291054. We also thank the ISOLDE collaboration for providing excellent beams.

[1] J. Wrzesiński *et al.*, Eur. Phys. J. A **10**, 259 (2001).
[2] M. Rejmund *et al.*, Eur. Phys. J. A **1**, 261 (1998).
[3] M. Rejmund *et al.*, Z. Phys. A **359**, 243 (1997).
[4] G. J. Lane *et al.*, Nucl. Phys. A **682**, 71c (2001).
[5] M. Pfützner *et al.*, Phys. Lett. B **444**, 32 (1998).
[6] H. Alvarez-Pol *et al.*, Phys. Rev. C **82**, 041602(R) (2010).
[7] A. Gottardo *et al.*, Phys. Rev. Lett. **109**, 162502 (2012).
[8] G. Benzoni *et al.*, Phys. Lett. B **715**, 293 (2012).
[9] E. Kugler, Hyperfine Interact. **129**, 23 (2000).
[10] V. Fedosseev *et al.*, Nucl. Instrum. Methods Phys. Res. B **204**, 353 (2003).
[11] U. Köster, V. N. Fedoseyev, and V. I. Mishin, Spectrochim. Acta, Part B **58**, 1047 (2003).
[12] P. Van Duppen *et al.*, Nucl. Instrum. Methods Phys. Res. B **134**, 267 (1998).
[13] J. Kurpeta *et al.*, Eur. Phys. J. A **18**, 31 (2003).

[14] J. Kurpeta *et al.*, Eur. Phys. J. A **7**, 49 (2000).
[15] J. Kurpeta *et al.*, Eur. Phys. J. A **18**, 5 (2003).
[16] H. De Witte *et al.*, Phys. Rev. C **69**, 044305 (2004).
[17] E. Ruchowska, J. Zylicz, C. F. Liang, P. Paris, and Ch. Briancon, J. Phys. G **16**, 255 (1990).
[18] M. Dombsky and P. Bricault, Nucl. Instrum. Methods Phys. Res. B **266**, 4240 (2008).
[19] L. Weissman *et al.*, Nucl. Instrum. Methods Phys. Res. A **423**, 328 (1999).
[20] P. Möller, J. R. Nix, and K.-L. Kratz, At. Data Nucl. Data Tables **66**, 131 (1997).
[21] http://www.nndc.bnl.gov/ensdf/.
[22] http://www.nndc.bnl.gov/hsicc/.
[23] I. N. Borzov, Phys. Rev. C **67**, 025802 (2003).
[24] I. N. Borzov, E. E. Saperstein, S. V. Tolokonnikov, G. Neyens, and N. Severijns, Eur. Phys. J. A **45**, 159 (2010).
[25] I. N. Borzov, Phys. At. Nucl. **74**, 1435 (2011).
[26] J. Benlliure *et al.*, J. Phys.: Conf. Ser. **337**, 012070 (2012).
[27] B. Singh, J. L. Rodriguez, S. S. M. Wong, and J. K. Tuli, Nucl. Data Sheets **84**, 487 (1998).
[28] V. G. Chumin, V. I. Fominykh, K. Ya. Gromov, M. Ya. Kuznetsova, V. V. Tsupko-Sitnikov, and M. B. Yuldashev, Z. Phys. A **358**, 33 (1997).
[29] S. Rothe *et al.*, Nature Commun. **4**, 1835 (2013).
[30] K. A. Erb and W. S. Gray, Phys. Rev. C **8**, 347 (1973).
[31] W. Baldridge, N. Freed, and J. Gibbons, Phys. Lett. B **46**, 341 (1973).
[32] E. R. Flynn, R. E. Anderson, N. J. DiGiacomo, R. J. Peterson, and G. R. Smith, Phys. Rev. C **16**, 139 (1977).
[33] S. Franchoo *et al.*, Phys. Rev. C **64**, 054308 (2001).
[34] J. Shergur *et al.*, Phys. Rev. C **65**, 034313 (2002).
[35] T. Otsuka, T. Suzuki, R. Fujimoto, H. Grawe, and Y. Akaishi, Phys. Rev. Lett. **95**, 232502 (2005).
[36] L. Coraggio, A. Covello, A. Gargano, and N. Itaco, Phys. Rev. C **72**, 057302 (2005).
[37] L. Coraggio, A. Covello, A. Gargano, and N. Itaco, Phys. Rev. C **80**, 021305(R) (2009).